JOURNAL OF MATERIALS SCIENCE 26 (1991) 23–27

Residual stress measurement in filament-evaporated aluminium films on single crystal silicon wafers

HAI-WOONG PARK, S. DANYLUK
University of Illinois at Chicago, Department of Civil Engineering, Mechanics, and Metallurgy, PO Box 4348, MC 246 Chicago, Illinois 60680, USA

Shadow Moire interferometry was used to determine the residual stresses in thin, filament-evaporated aluminium films deposited on (100) p-type, 10.16 cm diameter, 0.05 cm thick, circular single crystal silicon wafers. The aluminium film thicknesses ranged from 70 to 780 nm. Benchmark experiments on wafers without aluminium films showed that wafers possess in-plane residual stresses; the centre of the wafer is under tensile stresses of the order of 30 MPa and these stresses decrease toward the edge of the wafers to approximately 10 MPa. The deposition of aluminium films increases these tensile residual stresses by 3 to 15 MPa depending on the film thickness. The increase in the stress is attributed to the stresses in the films.

1. Introduction

The influence of residual stresses on the processing and performance of microelectronic circuits has been the subject of extensive study for many years [1–4]. Out-of-plane residual stresses are known to cause buckling of semiconductor and ceramic substrates [5], produce interfacial stresses at substrate–metal and substrate–polymer interfaces so that debonding of these thin films results and, residual stresses can influence the yield of devices if the stresses initiate or contribute to the propagation of microcracks [6]. If residual stresses are of sufficient magnitude to produce deformation or induce defects, then the electrical properties may also be affected [7]. As the circuit density of integrated circuit devices increases and, with the advent of the design of micromachined sensors and micronmeter-sized machines, a knowledge of residual stresses has become of critical concern.

This paper describes experimental results of the in-plane residual stresses in thin aluminium films deposited by filament vapour deposition on circular single crystal wafers. A shadow Moire technique was used to measure the strains over large spatial areas and, the in-plane residual stresses were deduced by comparing the measured and predicted deflections of wafers with and without the thin aluminium films. The stress calculation depends on an analysis of the edge effects of thin, short, flat plates.

2. Experimental procedure

Benchmark experiments were performed on two, 102 mm diameter, 0.5 mm thick, single crystal silicon wafers obtained from the Monsanto Electronic Materials Company. The wafers had one side polished and the other lapped according to semiconductor industry standards and each side contained a native oxide. The in-plane residual stresses were deduced from deflection measurements [8]. The wafers are mounted in a fixture so that a centrosymmetric load may be applied on the lapped side. The polished side was pressed against a knife edge of the fixture (as shown in Fig. 1) so that the outer edge is simply supported and, this polished side positioned in front of a 200 lines per inch grating with a grating thickness of 1.7 mm. This surface is illuminated by a helium–neon laser so that the grating casts a shadow on the surface. If the sample surface is non-planar as would be the case if a load was applied, then interference fringes are observed (as shown in Fig. 2). An analysis of the density and spacing of the fringes can be used to extract the sample topography, assuming that the geometry, such as the distance of the illumination source to the grating surface, is known.

After the benchmark experiments were complete, thin aluminium films were deposited on the silicon wafers by filament vacuum evaporation. The aluminium charge (99.99% purity) was loaded into a tungsten boat, the wafers were positioned in a fixture which was fixed at 15 cm from the evaporation source and the vacuum system evacuated to 5×10^{-6} torr. The fixture holding the wafers clamped the edges so that approximately 0.63 cm of the radius was shielded from the evaporation source. A d.c. current heated the tungsten boat so that the aluminium vapour was deposited on each wafer, one at a time, with the wafers not intentionally heated during the deposition. The surface temperature was measured in separate duplicate experiments and the temperature was measured to be 60 °C.

The deposition was done in three steps. The first

0022–2461/91 $03.00 + .12

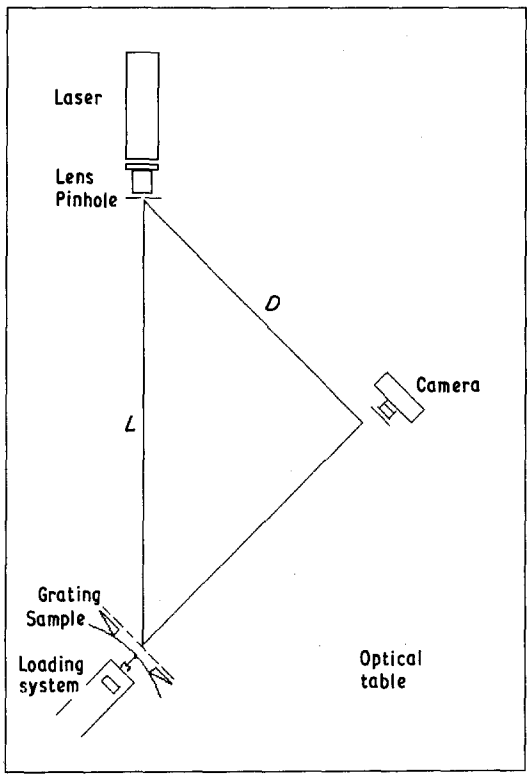

Figure 1 The schematic diagram for the shadow Moire experimental arrangements.

aluminium layer was deposited and the stresses were measured. After these measurements, the wafer was reloaded into the vacuum system and an additional aluminium layer was deposited and so on, until thicknesses of 70 and 180 nm were produced on wafer 1 and, 130, 405 and 780 nm were produced on wafer 2. The aluminium film thickness was measured by a multiple beam interferometer using the edge of the

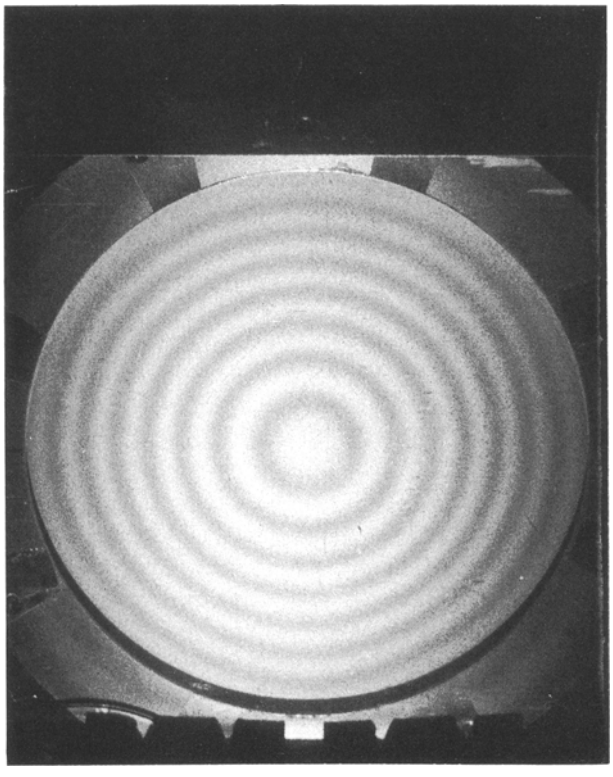

Figure 2 An example of an interferrogram fringe pattern of a circular plate.

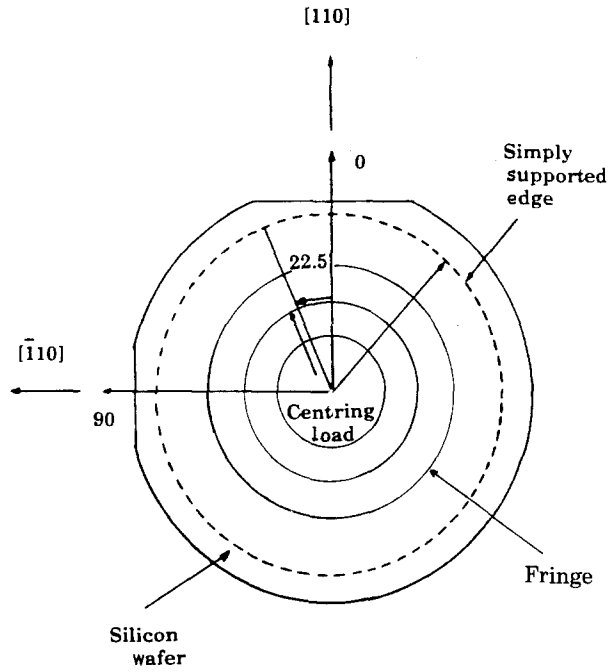

Figure 3 Wafer orientation and reading direction.

aluminium film and by Rutherford backscattering. The thicknesses were found to agree to within 10% from the centre to the edge of the wafer.

The strain measurements are performed by loading the silicon wafer so that it forms a dome shape. This produces a "bullseye" interference pattern and the interference fringes were measured along sixteen radial lines, from the centre out towards the outer edge as shown in Fig. 3. Since the wafers are single crystals, the 0° and 90° orientations are along the [110] and [$\bar{1}$10], respectively.

3. Results and discussion

An analysis of the deflection of centro-symmetrically loaded, thin circular plates has been previously published [8] and we have used the analytical results of that work to analyse the present data. The theoretical deflection, w, of a simply supported circular plate, loaded at the centre can be expressed as

$$w = \frac{P}{16\pi D}\left[\frac{3 + \nu}{1 + \nu}(a^2 - r^2) + 2r^2 \ln\left(\frac{r}{a}\right)\right]$$

where P is the load, a and r the radius and the distance from the centre, respectively, ν Poisson's ratio and D the flexural rigidity defined by

$$D = \frac{Eh^3}{12(1 - \nu^2)}$$

where E is Young's modulus and h the sample thickness. The deflection, w, is obtained at discrete points on the sample surface where fringe lines are measured. These data points are used in a cubic spline subroutine [9] to generate an analytical curve of the deflection of the entire sample. The equation for the deflection may then be rewritten as

$$w(r) = Ar^2 \ln\left(\frac{r}{a}\right) + Br^2 + C$$

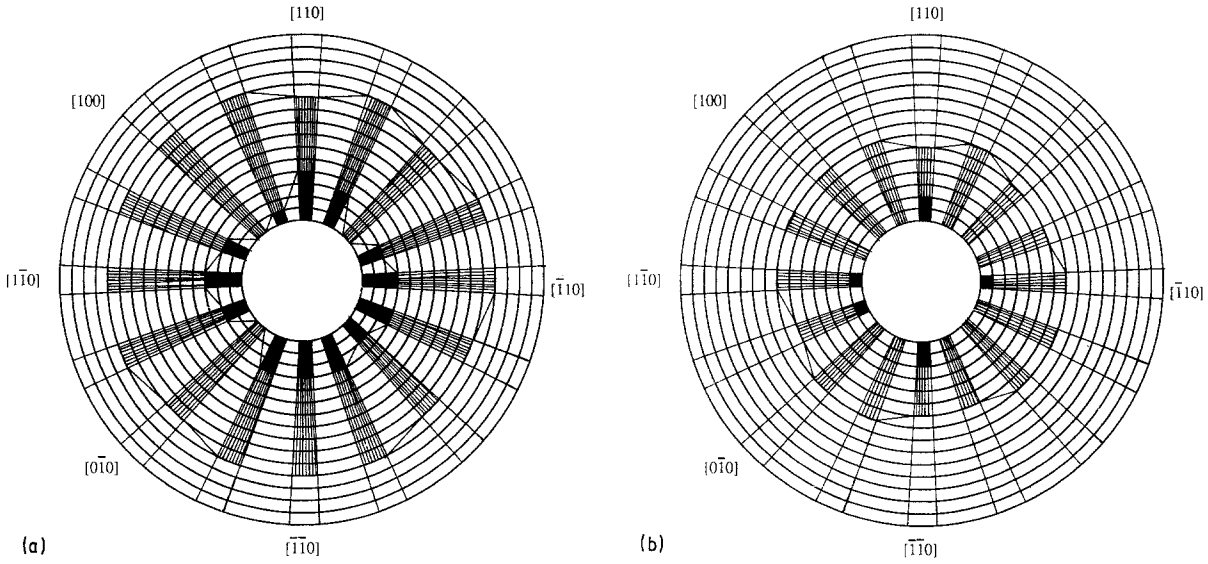

Figure 4 In-plane stress distribution before aluminium deposition for samples (a) 1 and (b) 2. (□ < 20.0 MPa, ▥ 20.1–30.0 MPa, ■ > 30.1 MPa).

where A, B and C incorporate the material parameters and these are obtained from fitting the experimental data to the analytical form of the deflection curve.

The residual stresses may be calculated if the first, second and third derivatives of the deflection are obtained experimentally. The equation relating the radial component of the in-plane residual stress, $N(r)$, to these derivatives is

$$N(r) = \left(\frac{dw}{dr}\right)^{-1} \times \left[D\left(\frac{d^3w}{dr^3} + \frac{1}{r}\frac{d^2w}{dr^3} - \frac{1}{r^2}\frac{dw}{dr}\right) - \frac{P}{2\pi r}\right]$$

$N(r)$ can thus be determined since the derivatives of the deflection and the load are known.

An example of the in-plane residual stress distribution of a wafer prior to the deposition of an aluminium film is shown in Fig. 4. This figure shows three regions of stress; the inner region contains tensile stresses greater than 30 MPa, the central region has stresses between 20 and 30 MPa and, the outer region has stresses from 10 to 20 MPa. There does not appear any obvious correlation of these stress distributions to the crystallographic directions. The stresses of this wafer changed when the surface was coated with an aluminium film and Fig. 5 shows the sequence of in-plane residual stress distributions as a function of aluminium film thickness. The residual stresses increase and expand over the surface. For example, within 1 cm of the centre, the stresses fall in the range of 30 MPa. With a film of thickness 180 nm the stresses expand to cover one quarter of the wafer. Similar data for the second wafer are shown in Fig. 6.

The data shown in Figs 5 and 6 have been replotted in Figs 7 and 8 along the [110] for the two wafers to dramatize the increase in the residual stresses as the aluminium film thickness increases. For any thickness, the stresses decrease monotonically from the centre toward the outer edge, however, the stresses increase

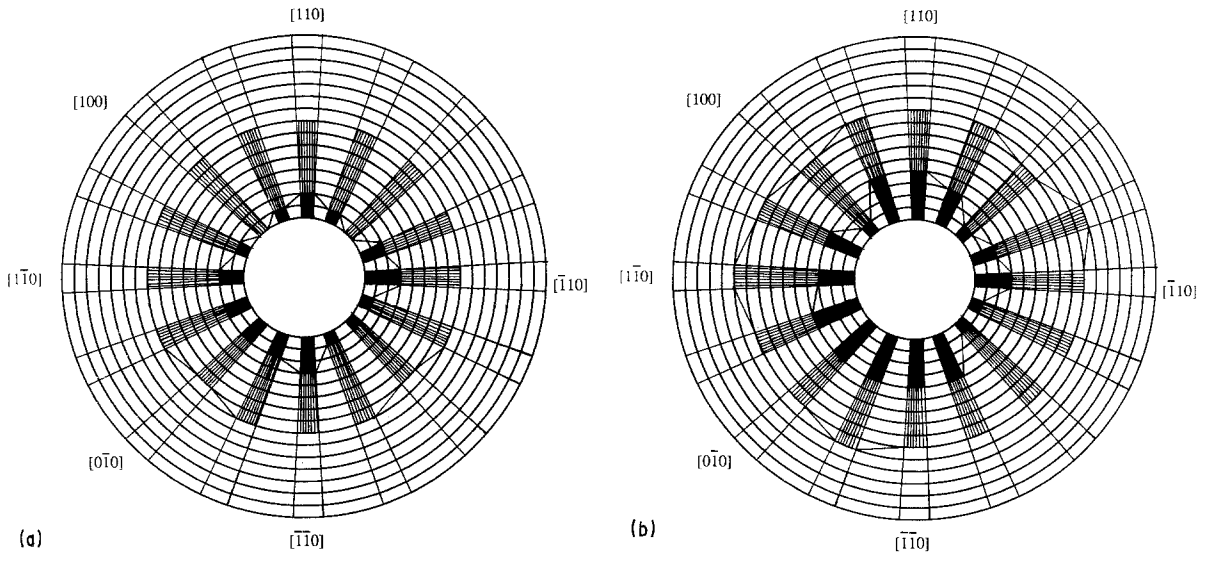

Figure 5 In-plane stress distribution for sample 1. (a) 70 nm, (b) 180 nm. Symbols as in Fig. 4.

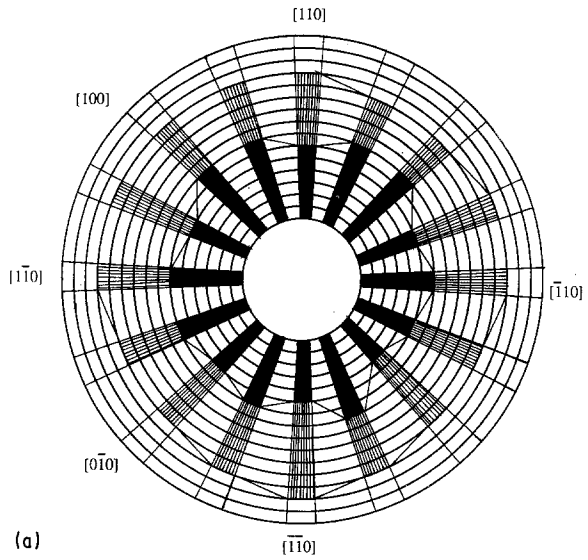

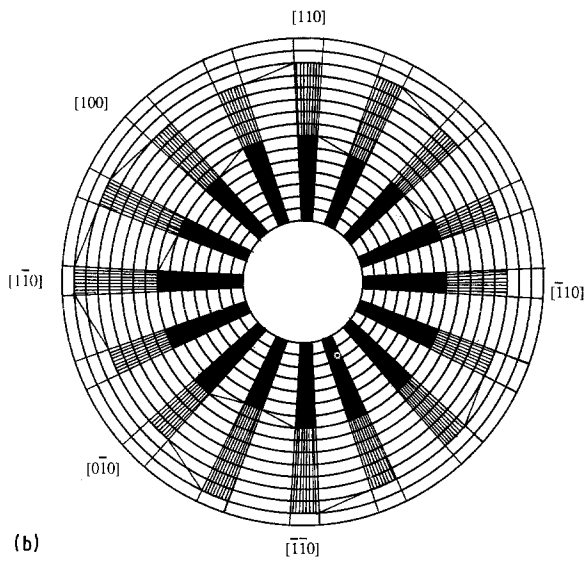

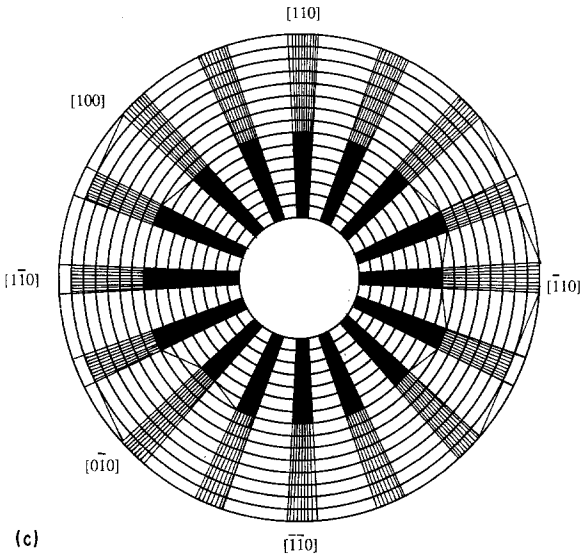

Figure 6 In-plane stress distribution for sample 2. (a) 130 nm, (b) 405 nm, (c) 780 nm. Symbols as in Fig. 4.

systematically as the aluminium film thickness is increased. The relative increase in residual stresses ranges from 19 to 32%. This change in stress against film thickness is plotted in Fig. 9. As can be seen, the increase appears to vary parabolically and approach saturation.

A number of previous workers have attributed the changes in residual stresses in metallic films on substrates to lattice mismatch between the substrate and the film [10, 11], the incorporation of gaseous impurities during the deposition of the film [12] and the growth of oxide [13] and recrystallization and grain growth of the film during heat treatments [14]. Our experimental conditions generate a multilayer film

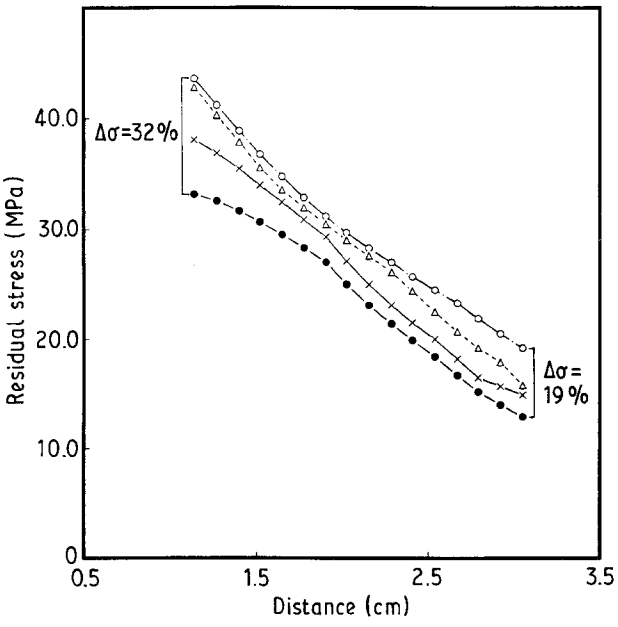

Figure 7 In-plane stress as a function of radial distance for various values of film thickness in [110] direction (sample 2). (● without film, × 130 nm, △ 405 nm, ○ 780 nm).

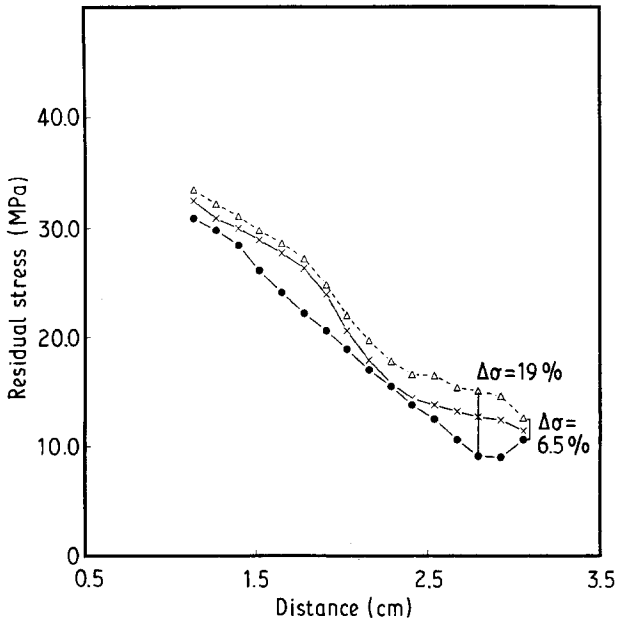

Figure 8 In-plane stress as a function of radial distance for various values of film thickness in [110] direction. (● without film, × 70 nm, △ 180 nm).

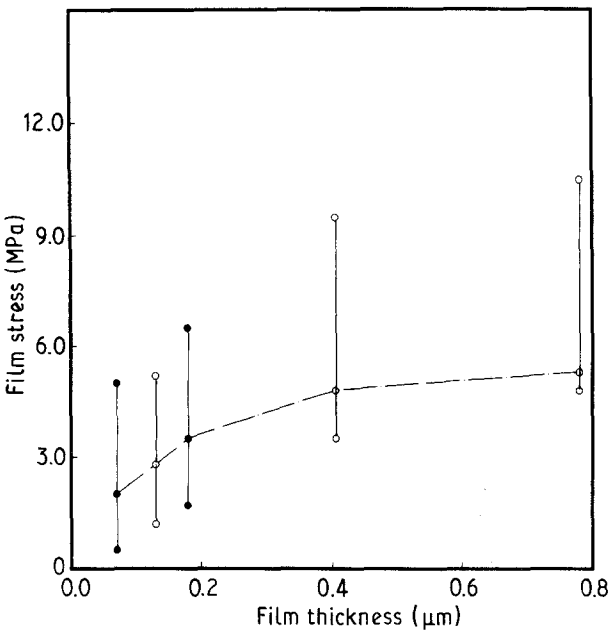

Figure 9 The variation of stress as a function of film thickness in [110] direction. (● sample 1, ○ sample 2).

since the aluminium oxidizes, and each measurement is the sum of the stresses of these layers. We have not yet characterized these films by microchemical techniques so it is not possible to identify the causes of the stresses. This characterization is continuing and will be reported shortly.

Acknowledgements

This work was supported in part by the Mobil Solar Energy Corporation. We thank Dr Juris Kalejs for his encouragement and interest throughout the course of this study. The silicon wafers were provided by Monsanto Electronics Materials Co. Special thanks also go to M. McGuire, Y. Im, and J. Gramsas of UIC and, Dr Y. Kwon of the Korean Standards Research Institute.

References

1. E. KLOKHOLM and J. E. FREEDMAN, *J. Appl. Phys.* **38** (1967) 1354.
2. G. KOPPELMANN and H. LEYENDECKER, *Optik* **25** (1967) 85.
3. D. S. RICKERBY, G. ECKOLD, K. T. SCOTT and I. M. BUCKLEY-GOLDER, *Thin Solid Film* **125** (1987) 154.
4. S. T. AHN, H. W. KENNEL, J. D. PLUMMER and W. A. TILLER, *J. Appl. Phys.* **64** (1988) 15.
5. L. T. TONCHEVA, *Crys. Latt. Def. Amorph. Mater.* **10** (1983) 89.
6. V. M. KOLESHKO, V. F. BELITSKY and I. V. KIRYUSHIN, *Thin Solid Films* **199** (1986) 142.
7. S. ISOMAE, *J. Appl. Phys.* **52** (1981) 2782.
8. A. T. ANDONIAN and S. DANYLUK, *Mech. Res. Commun.* **11** (1984) 97.
9. R. E. ROWLANDS, T. LIBER, I. M. DANIAL and P. G. ROSE, *Exp. Mech.* **105** (1973) 785.
10. J. H. VANDER MERWE, *J. Appl. Phys.* **34** (1963) 123.
11. J. W. MATTHEWS and E. GRUNBAUM, *Phil. Mag.* **11** (1965) 1233.
12. P. CHAUDHARI, *J. Vac. Sci. Tech.* **9** (1972) 520.
13. A. KUBOVY and M. JANDA, *Thin Solid Film* **42** (1977) 169.
14. C. VAN OPDORP and M. J. VERKERK, *J. Appl. Phys.* **63** (1988) 1518.

Received 15 May
and accepted 20 October 1989